Физика конденсированного состояния

Condensed state physics

УДК 538.91

СТРУКТУРНО-ФАЗОВОЕ СОСТОЯНИЕ ЗАЭВТЕКТИЧЕСКОГО СИЛУМИНОВОГО СПЛАВА Al – 20Si ПОСЛЕ ВОЗДЕЙСТВИЯ КОМПРЕССИОННЫМИ ПЛАЗМЕННЫМИ ПОТОКАМИ

В. И. ШИМАНСКИЙ[1)]***, А. ЕВДОКИМОВС***[1)]***,***
Н. Н. ЧЕРЕНДА[1)]***, В. М. АСТАШИНСКИЙ***[2)]***, Е. А. ПЕТРИКОВА***[3)]

[1)]*Белорусский государственный университет, пр. Независимости, 4, 220030, г. Минск, Беларусь*
[2)]*Институт тепло- и массообмена им. А. В. Лыкова НАН Беларуси,*
ул. П. Бровки, 15, 220072, г. Минск, Беларусь
[3)]*Институт сильноточной электроники, Сибирское отделение РАН,*
пр. Академический, 2, корп. 3, 634055, г. Томск, Россия

Образец цитирования:
Шиманский ВИ, Евдокимовс А, Черенда НН, Асташинский ВМ, Петрикова ЕА. Структурно-фазовое состояние заэвтектического силуминового сплава Al – 20Si после воздействия компрессионными плазменными потоками. *Журнал Белорусского государственного университета. Физика.* 2021;2:25–33 (на англ.).
https://doi.org/10.33581/2520-2243-2021-2-25-33

For citation:
Shymanski VI, Jevdokimovs A, Cherenda NN, Astashynski VM, Petrikova EA. Structure and phase composition of hypereutectic silumin alloy Al – 20Si after compression plasma flows impact. *Journal of the Belarusian State University. Physics.* 2021; 2:25–33.
https://doi.org/10.33581/2520-2243-2021-2-25-33

Авторы:
Виталий Игоревич Шиманский – кандидат физико-математических наук, доцент; доцент кафедры физики твердого тела физического факультета.
Антонс Евдокимовс – студент физического факультета. Научный руководитель – В. И. Шиманский.
Николай Николаевич Черенда – кандидат физико-математических наук, доцент; доцент кафедры физики твердого тела физического факультета.
Валентин Миронович Асташинский – член-корреспондент НАН Беларуси, доктор физико-математических наук; заместитель директора по научной работе и инновационной деятельности.
Елизавета Алексеевна Петрикова – младший научный сотрудник лаборатории плазменной эмиссионной электроники.

Authors:
Vitali I. Shymanski, PhD (physics and mathematics), docent; associate professor at the department of solid-state physics, faculty of physics.
shymanskiv@mail.ru
https://orcid.org/0000-0003-2956-3328
Antons Jevdokimovs, student at the faculty of physics.
jevdokimovanton@gmail.com
https://orcid.org/0000-0002-4577-7230
Nikolai N. Cherenda, PhD (physics and mathematics), docent; associate professor at the department of solid-state physics, faculty of physics.
cherenda@bsu.by
https://orcid.org/0000-0002-2394-5117
Valiantsin M. Astashynski, corresponding member of the National Academy of Sciences of Belarus, doctor of science (physics and mathematics); vice-director on science and innovations.
ast@hmti.ac.by
https://orcid.org/0000-0001-5297-602X
Elizaveta A. Petrikova, junior researcher at the laboratory of plasma-emission electronics.
elizmarkova@yahoo.com
https://orcid.org/0000-0002-1959-1459

В работе представлены результаты исследования структуры и фазового состава заэвтектического силуминового сплава с содержанием кремния 20 ат. % после высокоэнергетического импульсного воздействия компрессионными плазменными потоками. Обнаружено, что при воздействии плазменными потоками с режимами, обеспечивающими плотность поглощаемой энергии 25–40 Дж/см^2, происходит модифицирование приповерхностного слоя сплава толщиной до 30–32 мкм, в котором реализуются процессы плавления и последующего скоростного охлаждения. С помощью рентгеноструктурного анализа установлено, что в модифицированном слое заэвтектического силуминового сплава формируется мелкокристаллическая фаза кремния, присутствующая в эвтектической смеси Al – Si, а также крупнокристаллическая фаза кремния, представленная первичными кристаллами. Полученные результаты позволяют разработать способ наноструктурирования кремния в заэвтектических силуминах для повышения износостойкости изготовляемых изделий.

Ключевые слова: заэвтектический силуминовый сплав; кремний; модифицирование поверхности; компрессионные плазменные потоки; рентгеноструктурный анализ; микронапряжения.

Благодарность. Работа выполнена в рамках международного проекта при финансовой поддержке Белорусского республиканского фонда фундаментальных исследований и Российского фонда фундаментальных исследований (проект № Т19РМ-091).

STRUCTURE AND PHASE COMPOSITION OF HYPEREUTECTIC SILUMIN ALLOY Al – 20Si AFTER COMPRESSION PLASMA FLOWS IMPACT

***V. I. SHYMANSKI*[a], *A. JEVDOKIMOVS*[a], *N. N. CHERENDA*[a], *V. M. ASTASHYNSKI*[b], *E. A. PETRIKOVA*[c]**

[a]*Belarusian State University, 4 Niezaliežnasci Avenue, Minsk 220030, Belarus*
[b]*A. V. Luikov Heat and Mass Transfer Institute, National Academy of Sciences of Belarus, 15 P. Broŭki Street, Minsk 220072, Belarus*
[c]*Institute of High-Current Electronics, Siberian Branch of the Russian Academy of Sciences, 2 Akademicheskii Avenue, 3 building, Tomsk 634055, Russia*
Corresponding author: V. I. Shymanski (shymanskiv@mail.ru)

The results of structure and phase composition investigation in hypereutectic silumin alloy with 20 at. % Si content after high-energy pulsed compression plasma flows impact are presented in the work. The compression plasma flows impact with an absorbed energy density 25–40 J/cm^2 allows to modify the sub-surface layer with a thickness up to 30–32 μm due to its melting and high rate solidification. By means of X-ray diffraction method, it was found the formation of two silicon phases with different grain sizes. The high-dispersed structure of silicon is presented in the Al – Si eutectic while the silicon phase with coarse grains exists in the primary crystals. The obtained results are the basis for a new method development for nanostructuring of the surface layers of hypereutectic silumin alloys increasing its wear resistance.

Keywords: hypereutectic silumin alloy; silicon; surface modification; compression plasma flows; X-ray diffraction; microstrains.

Acknowledgements. This work was supported by the Belarusian Republican Foundation for Fundamental Research and Russian Foundation for Basic Research (project No. T19PM-091).

Introduction

Aluminum- and silicon-based alloys (silumins) are widespread materials in machining, aviation, household appliance production. Moreover, silumins are the main materials for pistons of internal combustion engines. Such wide range of silumins usages is due to low specific weight, high wear resistance and good casting properties. In dependence on silicon content the silumins are divided in three main groups: i) hypoeutectic alloys (Si content is less than 12 at. %), ii) eutectic alloys (Si content is 12–13 at. %) and iii) hypereutectic alloys (Si content is more than 13 at. %). Though, the hypoeutectic and eutectic alloys have more practical applications, increase in Si content more than 13 at. %, i. e. transition to the hypereutectic region of the alloys, will allow to rise wear resistance of the details and decrease its thermal expansion coefficient [1–7]. It makes the hypereutectic Al – Si alloys more promising materials for practical purposes.

Nevertheless, the usage of the Al – Si alloys with a high Si concentration has some difficulties and limitations connected to presence of coarse particles of primary silicon which are sources of the internal mechanical stress. The particles of primary silicon result in destroying of the material during exploiting. Besides, aluminum and silicon have limited mutual solubility in solid phase that is a reason of pores formation after casting. When being in liquid phase, donor-acceptor bond arises between aluminum and silicon atoms that results in growth of strong bonded silicon clusters. The electron density around the silicon atoms rises and prevents from the penetration other silicon atoms into the clusters. So, the excess in silicon atoms is deleted from the liquid solution, and the primary silicon crystals grow. Due to different values of the thermal expansion coefficient of silicon and aluminum-silicon eutectic mixture there is a lot of pores in the solidified structure of silumin alloy. High porosity degrades the mechanical properties of the Al – Si alloy, which makes it difficult to use. To solve this problem, the silumins are alloyed with different elements to reduce the heterogeneity of the structure. For example, Mg is used because of formations of silicide Mg_2Si which dissolves during annealing and the elements forming it diffuse into a solid solution. After aging, dispersed particles are released and provide the hardening effect.

In this work, it is proposed to use the method of surface treatment with a high-energy compression plasma flow for a hypereutectic silumin alloy obtained by the traditional casting method. The high-energy pulsed plasma exposure is known to melt the near-surface layer of the sample for homogenising the elemental composition and forming nonequilibrium phases as oversaturated solid solutions and intermetallic compounds after nonequilibrium crystallisation conditions [8–10]. The described phenomena make it possible to improve the mechanical characteristics of the modified alloy and increase its wear resistance. The structure state of the hypereutectic silumin alloy with Si content of 44 at. % (Al – 44Si) was modified that was described in [11].

The main aim of this work was to find the main features of structure changes in a hypereutectic silumin alloy containing 20 at. % of silicon caused by the action of compression plasma flows with different densities of absorbed energy.

Experimental

The objects of the study were samples of the hypereutectic silumin alloy with a silicon content of 20 at. % (Al – 20Si) in the form of round plates with a diameter of 30 mm and a thickness of 2 mm. The samples were made by casting processes [12].

The surface of the plates was subjected to the action of compression plasma flows (CPF) generated in a magnetoplasma compressor of compact geometry. The treatment was carried out in the residual gas mode when the previously evacuated vacuum chamber was filled with a plasma-forming gas (nitrogen) to a pressure of 1.3 kPa (10 Torr). By varying the distance (L) between the sample surface and the electrodes from 6 to 14 cm, as well as varying the voltage across the capacitor system from 3.0 to 4.0 kV, the energy density absorbed by the sample surface layer (Q) was changed. The surface was modified by three successive pulses to make the influence more uniform. The duration of each pulse was 100 μs and the interval between them was 10–15 s.

The phase composition of the modified samples was determined using X-ray diffraction analysis on the Ultima IV diffractometer (*Rigaku*, Japan) in the Bragg – Brentano geometry (θ–2θ geometry) using a copper radiation ($\lambda = 0.154\,178$ nm). Registration of the X-ray diffraction patterns was carried out at a detector movement speed of 2 degrees per minute and the discreteness of the intensity registration was 0.05 degrees. The analysis of the surface morphology and microstructure of cross-sectional sections of the hypereutectic silumin alloys after the CPF influence was carried out using optical microscopy on the MI-1 microscope (Belarus).

Results and discussions

The interaction of the compression plasma flow with the surface of a solid can be explained by a liquid model [13], in which the plasma flow is considered as a continuous medium flowing around the surface of the sample. In this case, there is a partial transition of the plasma flow energy to the thermal energy of the solid target. It is the heat energy that provides heating of the near-surface layer of the material and controls the structural changes in it. To determine the value of the absorbed energy density, calorimetric studies were carried out on the samples of unalloyed aluminum. The results of calorimetric tests are shown in fig. 1. It can be seen from the obtained data that the values of the voltage on the capacitors system in the magnetoplasma compressor used in the experiment as well as the distances L, provide the density of the absorbed energy in the range from 25 to 40 J/cm^2, which are enough for melting the near-surface layer. When the plasma flow moves to the surface of the sample, at the moment of interaction with a target, the plasma spreads over the surface resulting in mixing of the melted state due to its tangential velocity. Because of hydrodynamic motion of the melt, the components of the Al – Si alloy, being in a liquid state, are mixed to each other resulting in homogenisation of the elemental composition. After

finishing of the plasma pulse, fast crystallisation with a high cooling rate of the molten near-surface layer takes place due to intense heat transfer towards the unmelted volume. The hydrodynamic mixing of the components of the hypereutectic silumin alloy and its subsequent fast crystallisation prevent from the silicon localisation in coarse grains and reduce the size of the primary crystals.

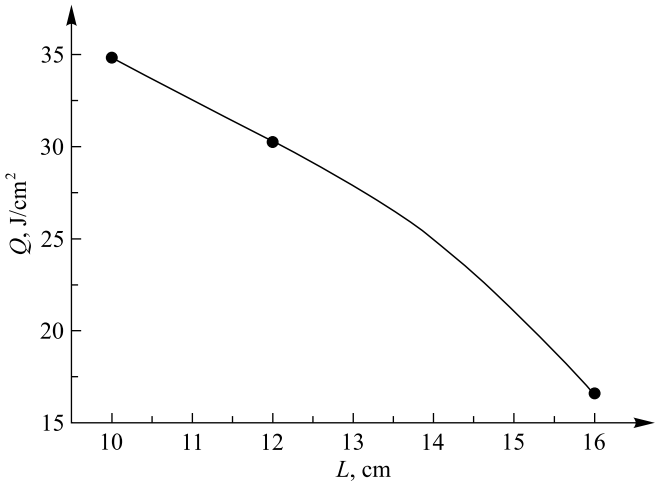

Fig. 1. Dependence of the absorbed energy density in the surface layer of aluminum on the distance between the sample and electrode during the CPF impact ($U = 4.0$ kV)

The thickness of the melted layer in the silumin alloys after plasma treatment was determined by means of optical microscopy (fig. 2). The near-surface homogeneous layer with a constant thickness is clearly visible on the images. This layer was formed after crystallisation and has a thickness of 30–32 μm for the samples treated with CPF at $U = 4.0$ kV and L is equal 6 and 10 cm ($Q = 35$–40 J/cm^2), and about 25 μm for the samples treated at $U = 4.0$ kV and $L = 14$ cm ($Q = 25$ J/cm^2). A fall in the depth of the melted layer with a decrease in the absorbed energy density is a result of the lower temperature reached on the surface of the silumin alloy specimen. It should be noted that there are no any coarse inclusions of primary silicon in the melted layer. Such inclusions are clearly visible in the structure of the initial state of the alloy (underneath of the modified layer).

The phase composition of the silumin samples after the CPF treatment was determined by means of X-ray diffraction (XRD) analysis (fig. 3 and 4). According to the obtained XRD patterns, only two phases (silicon and aluminum) were revealed in the analysed near-surface layer of the hypereutectic silumin alloy treated by the CPF at all used regimes.

The depth (H) of the layer analysed by the X-ray diffraction is calculated by the following expression [14]:

$$H = \frac{K}{\mu}\frac{\sin(2\theta - \alpha)\sin\alpha}{\sin(2\theta - \alpha) + \sin\alpha}, \quad (1)$$

where K is the constant value ($K = 5$); μ is the linear coefficient of the X-rays absorption; θ is the diffraction angle; α is the incident angle. For the silumin alloy as a composite material the linear absorption coefficient μ was calculated as an effective value additively taking into account the contribution of each element: $\mu = 0.2\mu_{Si} + 0.8\mu_{Al}$. After calculation the effective coefficient equals to $\mu = 1.34 \cdot 10^{-2}$ μm^{-1}. In the experiments we used the symmetric mode of the X-ray registration, therefore the condition $\alpha = \theta$ was satisfied, and the expression (1) can be written in the following form:

$$H = \frac{K\sin\theta}{2\mu}. \quad (2)$$

Thus, the depth of the analysed layer with X-ray beam ranges from 30 μm (at low diffraction angles) to 140 μm (at large diffraction angles). From a comparison of the obtained values to the depth of the melted layer (see fig. 2) it can be seen that the diffraction lines registered at small diffraction angles correspond to crystallographic reflections in the phases contained mainly in the melted modified layer. However, the diffraction lines at large diffraction angles are superpositions of the reflections from both the modified near-surface melted layer and the underlying unmodified layer. In this regard, for further analysis of the CPF effect on the structure of the silumin alloy we used diffraction lines at small diffraction angles.

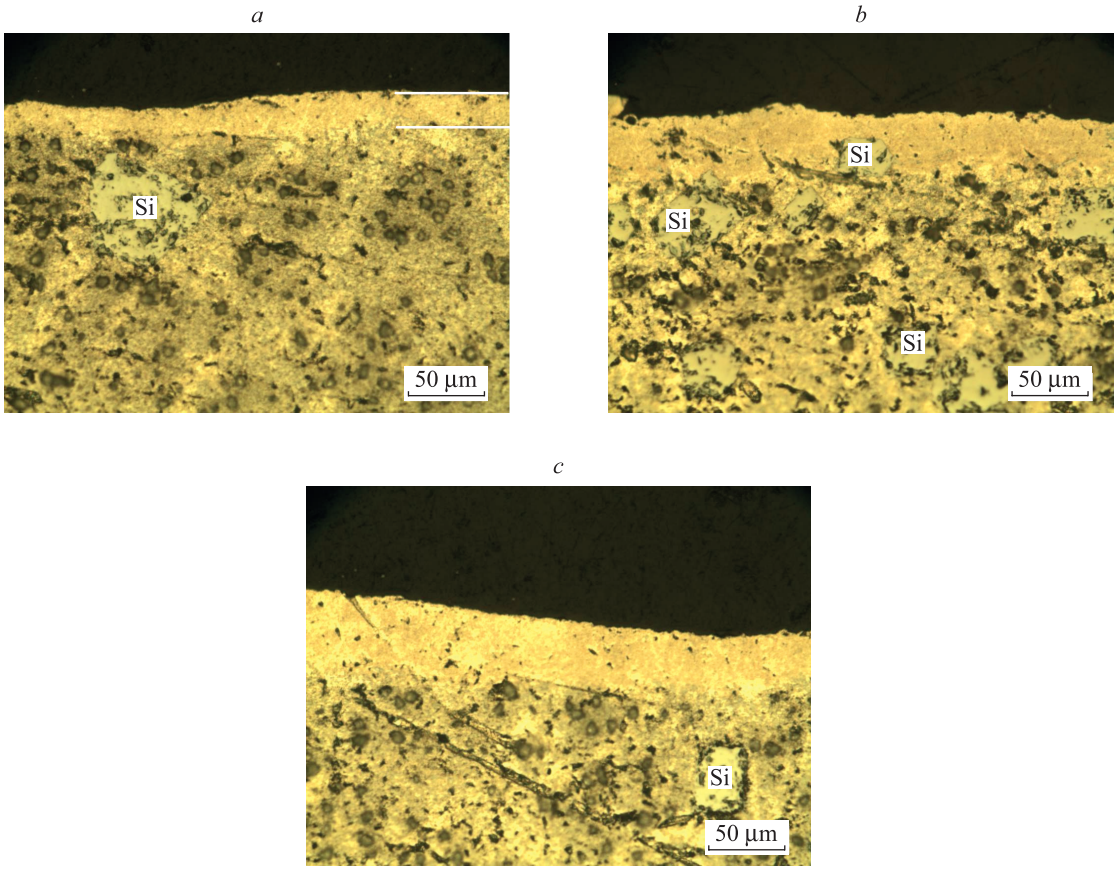

Fig. 2. Optical images of the cross-sections of the samples of Al – 20Si alloy after CPF impact at $U = 4.0$ kV and L is equal 14 cm (*a*), 10 cm (*b*), 6 cm (*c*). The primary crystals of silicon are detected on the pictures

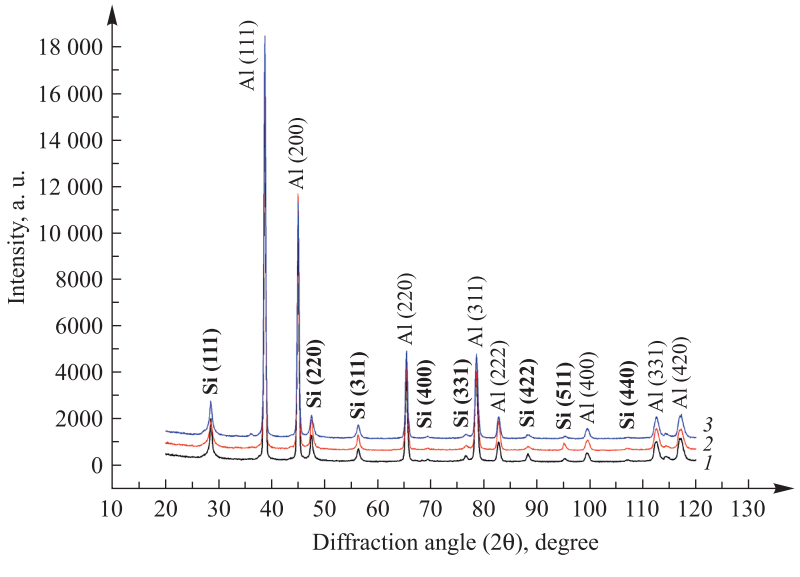

Fig. 3. XRD patterns of the Al – 20Si alloy after the CPF impact at $U = 4.0$ kV as-received state (*1*), and L is equal 14 cm (*2*), 10 cm (*3*), 6 cm (*4*)

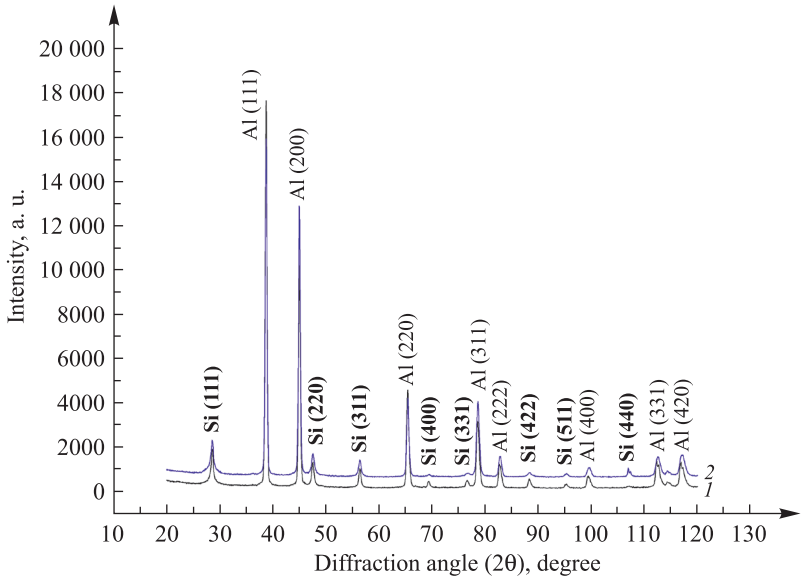

Fig. 4. XRD patterns of the Al – 20Si alloy
after the CPF impact at $U = 3.0$ kV and L is equal 14 cm (*1*), 6 cm (*2*)

A detailed analysis of the diffraction lines of silicon, for example, the lines (111), (220) or (311) of the silumin alloy samples after the CPF impact allows to notice their broadening which is especially clearly manifested near the base of the diffraction lines. The mathematical deconvolution of the experimentally obtained diffraction lines according to Gaussian curves shown that they are a superposition of two diffraction lines, each of them referring to reflections from the crystallographic planes of silicon, but with different widths at half maximum (fig. 5). It should be noted that such broadening of diffraction lines is not observed on the X-ray diffraction patterns of the initial sample that indicates the effect of plasma exposure and is associated with the effect of melting and crystallisation of the near-surface layer. It can be seen from the obtained X-ray diffraction patterns that the surface melting of the Al – 20Si silumin alloy occurs under all selected modes of the plasma exposure. The detected shape of the diffraction lines of silicon indicates its presence in two phase states. During the crystallisation of a hypereutectic silumin alloy, an eutectic mixture containing silicon and aluminum as well as the primary silicon crystallites is known to be formed. The amount of the primary crystals is determined by the excess of the silicon concentration in comparison with the eutectic composition: $(Al + Si) \rightarrow (AlSi)_{eut} + Si_{(I)}$. Then, it can be assumed that two detected silicon phases are silicon presented in both eutectic Si_{eut} and primary crystallites $Si_{(I)}$.

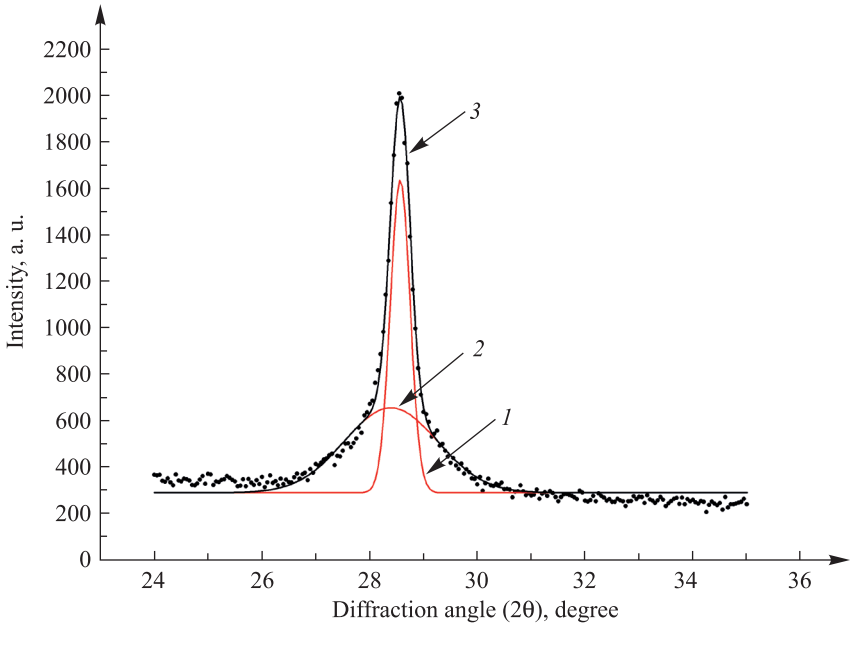

Fig. 5. Fitting of the (111) Si diffraction line of the Al – 20Si alloy after the CPF impact:
1 – the component of the silicon with coarse grains; *2* – the component of the silicon with dispersed grains;
3 – superposition of two components (the points show the experimental curve)

The broadening of diffraction lines is known to be mainly caused by two factors: i) the dispersion of the grain size; ii) the residual mechanical microstresses. Both of these factors introduce the additive contribution to the total broadening. The Williamson – Hall method can be used to separate these effects [15; 16]. According to this method, the microdeformation of the crystal lattice ε and the size of the coherent scattering blocks D, the real broadening of the diffraction line β, as well as the diffraction angle θ are related to each other by the following expression:

$$\beta\cos\theta = \frac{\lambda}{D} + 4\varepsilon\sin\theta. \quad (3)$$

The real broadenings of the diffraction lines were determined as the difference between the full width at half maximum in the analysed samples and the instrumental line width of 0.08 degree. When plotting the functional dependence $\beta\cos\theta = f(\sin\theta)$, the sizes of the coherent scattering blocks D as well as the magnitude of the microstrains in the silicon crystal lattice were calculated. The results are presented in table.

Microstrains and dimensions of coherent scattering blocks in silicon phases

Mode of the CPF impact		Fine-crystalline silicon		Coarse-crystalline silicon	
U, kV	L, cm	ε, %	D, nm	ε, %	D, nm
4.0	14	–0.2	5.9	0.01	33
4.0	10	–0.5	4.7	0.08	53
4.0	6	–0.7	4.1	–0.03	24
3.0	14	–1.1	3.7	–0.1	23
3.0	6	–0.5	4.1	0.0002	26

According to the obtained results, one of the silicon phases is characterised by very small sizes of coherent scattering blocks, which are in the range from 3.7 to 5.9 nm (fine-crystalline silicon), while the sizes in the second silicon phase reach 53 nm (coarse-crystalline silicon).

The integral intensity of the diffraction line is determined by the volume fraction of the phase and is a product of a number of factors, including the structural, atomic, temperature factors, as well as the repeatability, absorption, and Lorentz factors [17]. All of these factors depend on the structure of the analysed phase, the diffraction angle and the properties of the atoms included in the phase. Two detected silicon phases (eutectic silicon Si_{eut} and silicon in the form of primary crystallites $Si_{(l)}$) have identical crystal structure and atomic composition, so, when analysing two diffraction lines located at the same diffraction angles, the ratio between their integral intensities can show the volume ratio of the phases in the analysed layer. As a result of estimation, the volume content of silicon with a coherent scattering blocks size of 3.7–5.9 nm is 11–12 % which corresponds to the eutectic concentration of silicon in the Al – Si alloy. Moreover, it indicates that it is silicon in the eutectic mixture that is formed in the nanocrystalline structure form (fine-crystalline silicon). The volume fraction of the primary silicon crystallites is 8–9 % and, according to the results presented in table 1, this silicon phase has larger coherent scattering blocks size. The effect of nanostructuring of silicon was also observed earlier in the silumin alloys of eutectic composition when exposed to pulsed electron beams [18]. Separation of the silicon crystallites both in the eutectic mixture and in the primary crystals is most likely associated with the effect of rapid crystallisation during cooling the melt after plasma exposure. The silicon in the eutectic mixture contacts with the aluminum which has a higher thermal conductivity compared to the silicon one. As a result, the rate of heat transfer from silicon crystallites in the eutectic mixture increases in comparable to the heat transfer in the primary silicon crystals. This effect provides a higher level of the dispersion in the eutectic mixture.

The lattice parameter of aluminum determined from the XRD results is 0.404 nm and does not depend on the value of the absorbed energy density of the CPF treatment.

However, the lattice parameter of primary silicon crystals $Si_{(l)}$ is 0.541 nm and is 0.545 nm for silicon in the eutectic mixture Si_{eut}. The standard value of the lattice parameter of silicon is 0.543 nm. The obtained values of the lattice parameters for silicon phases do not practically depend on the modes of the plasma impact. Thus, the effect of separation of silicon into two phases is observed, i. e. one phase has a reduced lattice parameter and the second one has an increased lattice parameter with respect to the standard value. First of all, when excluding the influence of point defects that can be present in both phases of silicon, we can expect the influence of aluminum atoms on the crystal structure of the silicon. Indeed, the atomic radius of aluminum is 143 pm, while it is 132 pm for silicon. Therefore, an increase in the lattice parameter of the fine-crystalline phase may occur due to the partial penetration of aluminum atoms into the silicon lattice, which are placed directly in the

eutectic mixture with alternating Si and Al phases. According to the equilibrium binary state diagram [19], the solubility of aluminum in silicon is extremely low and does not exceed 0.016 at. %, however, the nonequilibrium conditions of the crystallisation caused by the CPF action can lead to an increase in the solubility limit. In primary silicon crystals, the lattice parameter decreases with respect to the standard value that cannot be explained by the incorporation of larger aluminum atoms, and, therefore, the excess concentration of vacancies due to rapid quenching from the melt plays the main role.

The analysis of microstrains in each of the detected silicon phases (see table) showed that compressive deformation of 0.2–1.1 % appears in the fine-crystalline silicon phase, i. e. in silicon of the eutectic mixture. Their appearance can be associated with an increase in the lattice parameter due to the dissolution of aluminum atoms. In the coarse-crystalline silicon phase, the dissolution of aluminum does not occur and, as a result, the level of residual microstresses is significantly reduced.

Conclusions

Thus, the compression plasma flows with an absorbed energy density of 25–40 J/cm^2 influence on the surface of the hypereutectic silumin alloy Al – 20Si leads to the modification of the near-surface layer due to its melting on the depth of 32 μm and uniform redistribution of silicon and aluminum in it. As a result of rapid crystallisation and homogenisation of the elemental composition, silicon is separated into two phase components: i) silicon with a fine-crystalline structure (the coherent scattering block size up to 6 nm) presenting in the eutectic mixture, and ii) the silicon with a coarse-crystalline structure (the coherent scattering block size up to 50 nm) characterising the primary crystals. Due to the dissolution of aluminum atoms in the fine-crystalline phase of silicon in the eutectic mixture the silicon lattice parameter increases and residual compressive stresses from 0.2 to 1.1 % appear.

Библиографические ссылки

1. Афанасьев ВК, Прудников АН, Горшенин АВ. Технология получения слитков, деформированных заготовок и поршней из заэвтектического жаропрочного силумина и их свойства. *Обработка металлов.* 2010;3:28–31.

2. Попова МВ, Кибко НВ. Влияние обработки расплава на параметры микроструктуры и тепловое расширение силуминов с различным содержанием кремния. *Обработка металлов.* 2014;2:107–116.

3. Шадаев ДА, Предко ПЮ, Лебедева ТИ, Конкевич ВЮ, Кузнецов АО, Гневашев ДА и др. Влияние особенностей технологии плавления на состав и морфологию фаз заэвтектических силуминов. *Технология легких сплавов.* 2015;2:105–111.

4. Jeon JH, Shin JH, Bae DH. Si phase modification on the elevated temperature mechanical properties of Al – Si hypereutectic alloys. *Materials Science and Engineering: A*. 2019;748:367–370. DOI: 10.1016/j.msea.2019.01.119.

5. Guoqiang Lv, Yu Bao, Yufeng Zhang, Yunfei He, Wenhui Ma, Yun Lei. Effects of electromagnetic directional conditions on the separation of primary silicon from Al – Si alloy with high Si content. *Materials Science in Semiconductor Processing*. 2018;81: 139–148. DOI: 10.1016/j.mssp.2018.03.006.

6. Maowen Liu, Ruixiao Zheng, Wenlong Xiao, Xiaohui Yu, Qiuming Peng, Chaoli Ma. Concurrent enhancement of strength and ductility for Al – Si binary alloy by refining phase to nanoscale. *Materials Science and Engineering: A.* 2019;751:303–310. DOI: 10.1016/j.msea.2019.02.081.

7. Shi WX, Gao B, Tu GF, Li SW. Effect of Nd on microstructure and wear resistance of hypereutectic Al – 20 % Si alloy. *Journal of Alloys and Compounds*. 2010;508:480–485. DOI: 10.1016/j.jallcom.2010.08.098.

8. Shymanski VI, Cherenda NN, Uglov VV, Astashynski VM, Kuzmitski AM. Structure and phase composition of Nb/Ti system subjected to compression plasma flows impact. *Surface and Coatings Technology*. 2015;278:183–189. DOI: 10.1016/j.surfcoat. 2015.08.014.

9. Cherenda NN, Basalai AV, Shymanski VI, Uglov VV, Astashynski VM, Kuzmitski AM, et al. Modification of Ti – 6Al – 4V alloy element and phase composition by compression plasma flows impact. *Surface and Coatings Technology*. 2018;355:148–154. DOI: 10.1016/j.surfcoat.2018.02.048.

10. Shymanski VI, Uglov VV, Cherenda NN, Pigasova VS, Astashynski VM, Kuzmitski AM, et al. Structure and phase composition of tungsten alloys modified by compression plasma flows and high-intense pulsed ion beam impacts. *Applied Surface Science.* 2019;491:43–52.

11. Шиманский ВИ, Евдокимовс А, Углов ВВ, Черенда НН, Асташинский ВМ, Кузьмицкий АМ и др. Модификация структуры заэвтектического силуминового сплава Al – 44Si при воздействии компрессионных плазменных потоков. *Физика и химия обработки материалов.* 2021;1:40–50. DOI: 10.30791/0015-3214-2021-1-40-50.

12. Марукович ЕИ, Стеценко ВЮ. Получение отливок из заэвтектического силумина методом литья закалочным затвердеванием. *Литье и металлургия.* 2005;2–1:142–144.

13. Морозов АИ, редактор. *Физика и применение плазменных ускорителей.* Минск: Наука и техника; 1974. 394 с.

14. Анищик ВМ, Понарядов ВВ, Углов ВВ. *Дифракционный анализ.* Минск: Вышэйшая школа; 2011. 215 с.

15. Goncalves NS, Carvalho JA, Lima ZM, Sasaki JM. Size-strain study of NiO nanoparticles by X-ray powder diffraction line broadening. *Materials Letters*. 2012;72:36–38. DOI: 10.1016/j.matlet.2011.12.046.

16. Venkateswarlu K, Bose AC, Rameshbabu N. X-ray peak broadening studies of nanocrystalline hydroxyapatite by Williamson – Hall analysis. *Physica B: Condensed Matter.* 2010;405:4256–4261.

17. Русаков АА. *Рентгенография металлов.* Москва: Атомиздат; 1977. 480 с.

18. Иванов ЮФ, Петрикова ЕА, Тересов АД, Москвин ПВ, Будовских ЕА, Коваль НН и др. Наноструктурирование поверхности силумина эвтектоидного состава электронно-ионно-плазменными методами. *Известия высших учебных заведений. Физика.* 2013;56(1–2):98–102.

19. Лякишев НП, редактор. *Диаграммы состояния двойных металлических систем. Том 1.* Москва: Машиностроение; 1996. 992 с.

References

1. Afanasiev VK, Prudnikov AN, Gorshenin AV. Technology of reception of the ingots, the deformed preparations and pistons from hypereutectic heat resisting silumin and them properties. *Obrabotka metallov*. 2010;3:28–31. Russian.

2. Popova MV, Kibko NV. The influence of melt processing on the microstructure and thermal expansion of silumins with different silicon content. *Obrabotka metallov*. 2014;2:107–116. Russian.

3. Shadaev DA, Predko PYu, Lebedeva TI, Konkevich VYu, Kuznetsov AO, Gnevashev DA, et al. The effect of a melting technology on composition and morphology of hypereutectic silumin phases. *Tekhnologiya legkikh splavov*. 2015;2:105–111. Russian.

4. Jeon JH, Shin JH, Bae DH. Si phase modification on the elevated temperature mechanical properties of Al – Si hypereutectic alloys. *Materials Science and Engineering: A*. 2019;748:367–370. DOI: 10.1016/j.msea.2019.01.119.

5. Guoqiang Lv, Yu Bao, Yufeng Zhang, Yunfei He, Wenhui Ma, Yun Lei. Effects of electromagnetic directional conditions on the separation of primary silicon from Al – Si alloy with high Si content. *Materials Science in Semiconductor Processing*. 2018;81: 139–148. DOI: 10.1016/j.mssp.2018.03.006.

6. Maowen Liu, Ruixiao Zheng, Wenlong Xiao, Xiaohui Yu, Qiuming Peng, Chaoli Ma. Concurrent enhancement of strength and ductility for Al – Si binary alloy by refining phase to nanoscale. *Materials Science and Engineering: A.* 2019;751:303–310. DOI: 10.1016/j.msea.2019.02.081.

7. Shi WX, Gao B, Tu GF, Li SW. Effect of Nd on microstructure and wear resistance of hypereutectic Al – 20 % Si alloy. *Journal of Alloys and Compounds*. 2010;508:480–485. DOI: 10.1016/j.jallcom.2010.08.098.

8. Shymanski VI, Cherenda NN, Uglov VV, Astashynski VM, Kuzmitski AM. Structure and phase composition of Nb/Ti system subjected to compression plasma flows impact. *Surface and Coatings Technology*. 2015;278:183–189. DOI: 10.1016/j.surfcoat. 2015.08.014.

9. Cherenda NN, Basalai AV, Shymanski VI, Uglov VV, Astashynski VM, Kuzmitski AM, et al. Modification of Ti – 6Al – 4V alloy element and phase composition by compression plasma flows impact. *Surface and Coatings Technology*. 2018;355:148–154. DOI: 10.1016/j.surfcoat.2018.02.048.

10. Shymanski VI, Uglov VV, Cherenda NN, Pigasova VS, Astashynski VM, Kuzmitski AM, et al. Structure and phase composition of tungsten alloys modified by compression plasma flows and high-intense pulsed ion beam impacts. *Applied Surface Science.* 2019;491:43–52.

11. Shimanski VI, Evdokimovs A, Uglov VV, Cherenda NN, Astashinski VM, Kuzmitsky AM, et al. Structure modification of hypereutectic silumin alloy Al – 44Si under the compression plasma flows impact. *Fizika i khimiya obrabotki materialov.* 2021;1:40–50. Russian. DOI: 10.30791/0015-3214-2021-1-40-50.

12. Marukovich EI, Stetsenko VYu. Production of castings of hypereutectic silumin by means of casting by quenching hardening. *Lit'e i metallurgiya*. 2005;2–1:142–144. Russian.

13. Morozov AI, editor. *Fizika i primenenie plazmennykh uskoritelei* [Physics and application of plasma accelerators]. Minsk: Nauka i tekhnika; 1974. 394 p. Russian.

14. Anishchik VM, Ponaryadov VV, Uglov VV. *Difraktsionnyi analiz* [Diffraction analysis]. Minsk: Vyshjejshaja shkola; 2011. 215 p. Russian.

15. Goncalves NS, Carvalho JA, Lima ZM, Sasaki JM. Size-strain study of NiO nanoparticles by X-ray powder diffraction line broadening. *Materials Letters*. 2012;72:36–38. DOI: 10.1016/j.matlet.2011.12.046.

16. Venkateswarlu K, Bose AC, Rameshbabu N. X-ray peak broadening studies of nanocrystalline hydroxyapatite by Williamson – Hall analysis. *Physica B: Condensed Matter.* 2010;405:4256–4261.

17. Rusakov AA. *Rentgenografiya metallov* [Radiography of metals]. Moscow: Atomizdat; 1977. 480 p. Russian.

18. Ivanov YuF, Petrikova EA, Teresov AD, Moskvin PV, Budovskikh EA, Koval' NN, et al. Nanostructuring of hyperwutectic silumin surface by electron-ion-plasma methods. *Izvestiya vysshikh uchebnykh zavedenii. Fizika*. 2013;56(1–2):98–102. Russian.

19. Lyakishev NP, editor. *Diagrammy sostoyaniya dvoinykh metallicheskikh sistem. Tom 1* [State diagrams of binary metal systems. Volume 1]. Moscow: Mashinostroenie; 1996. 992 p. Russian.

Received 18.02.2021 / revised 01.04.2021 / accepted 07.04.2021.